

Measurement of Excitation of N₂, CO, and He by Electron Impact*

G. J. SCHULZ

Westinghouse Research Laboratories, Pittsburgh, Pennsylvania

(Received July 17, 1959)

The inelastic excitation of N₂ and CO by electron impact is studied using the trapped-electron method. In this method those electrons which have lost a portion of their initial energy in an inelastic collision are trapped in a potential well. Well depths up to 3 volts are used in the present experiment. The operation of the apparatus is checked for helium, where the shape of the excitation function is known accurately. The shape of the excitation function for metastable helium atoms obtained by the trapped-electron method is in good agreement with previous results. A large inelastic peak is observed at 2.3 ev in N₂ and 1.7 ev in CO. This phenomenon is discussed in terms of the formation of a temporary negative ion state of N₂ or CO and subsequent decay into various vibrational levels of the molecule. This model explains the sharp peak in both the elastic and inelastic cross section in N₂ and CO. Neither O₂ nor H₂ show such a sharp peak at low energies.

EXCITATION of molecules by electron impact can be studied by means of the trapped-electron method. Some aspects of this method have been described in a previous publication¹ which will be referred to as Part I. In this method, an electron beam traverses an electric and magnetic field configuration in which those electrons which have lost energy in an inelastic collision are prevented from reaching the electron beam collector by a potential well. These "trapped electrons" (also called "slow electrons" in Part I) are collected on the trapped-electron collector and are a measure of the inelastic cross section. This paper presents an extension of the technique described in Part I. With the present tube, measurements can be extended to a well depth of about 3 to 4 volts, whereas the results presented in Part I extended to a well depth of only 0.1 to 0.2 volt. This increased depth of the potential well enables us to study the excitation function of atoms up to 3 to 4 ev above the onset of excitation. The results in helium are reported in Sec. III. In the case of molecules, inelastic processes can be detected which could not be detected with a small well depth. The results obtained in N₂ and CO are discussed in Secs. IV and V.

I. APPARATUS

Two different tubes are used for this experiment. They are identical in the principle of operation and differ from each other in the magnetic field uniformity and in the length of the collision chamber. The original tube will be designated as Tube A and the improved version as Tube B. Following a general description of the method, the differences between the two experimental arrangements will be discussed.

A schematic diagram of the experimental arrangement is shown in Fig. 1. Electrons from the filament, *F*, pass through the electron gun (only the retarding plate, *P*₂, is shown) into the collision chamber and are collected on the electron beam collector *E*. A magnetic

field aligns the electron beam. The construction of the electron gun, and the vacuum technique used have been described previously.^{1,2} The electron gun employs the retarding potential difference method so that the effect of nearly monoenergetic electrons can be measured. The grid, *G*, is surrounded by the cylindrical collector, *M* (10-millimeter diameter). The potential on *M* is usually positive with respect to *G*. The grid is much coarser than that used in the tube described in Part I; ten gold-plated molybdenum wires of 0.06-mm diameter are strung between the end plates, forming a cylindrical screen six millimeters in diameter. A large fraction of the potential applied between the grid, *G*, and the cylindrical collector, *M*, penetrates into the center of the tube. The potential difference between the center of the tube and the collision chamber elec-

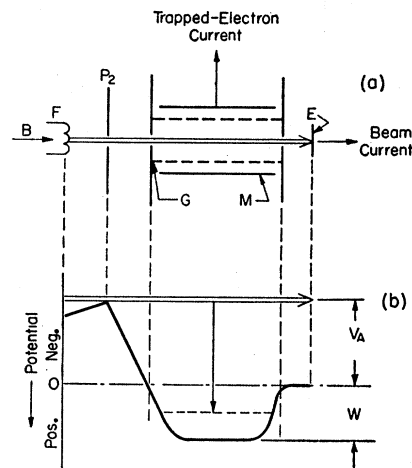


FIG. 1. Schematic diagram of tube and potential distribution at the axis of the tube. *F* is the filament, *P*₂ is the retarding electrode, *G* is the cylindrical grid forming the collision chamber, *M* is the cylinder for collection of trapped electrons, *E* is the electron beam collector. *V*_A is the accelerating voltage and *W* is the depth of the well. The double line in (b) indicates the energy of the electron beam and the arrow indicates the energy lost by an electron in an inelastic collision. The electron energy in the collision chamber is (*V*_A+*W*).

* This work has been supported in part by the Office of Naval Research.

¹ G. J. Schulz, Phys. Rev. **112**, 150 (1958). This paper will be referred to as Part I.

² G. J. Schulz and R. E. Fox, Phys. Rev. **106**, 1179 (1957).

trodes is the well depth and is denoted by W . Figure 1(b) shows, schematically, the potential vs the distance along the axis of the tube.

The length of the collision chamber in Tube A is 19 millimeters, that of Tube B is 152 millimeters. The increased length of the collision chamber should improve the uniformity of the well. A magnetron magnet with pole spacing of 5.5 centimeters and a flux density of 1000 gauss is used with Tube A and a solenoid supplying a flux density of 300 to 1000 gauss is used with Tube B . The more uniform magnetic field in Tube B forces the electrons to travel along the center of the tube so that the potential drop across the electron beam due to the variation of the well potential in the radial direction is minimized. This is especially important when high values of well depth are used. Experimental evidence for this improvement is discussed in the next section.

Another refinement of Tube B consists of plating the electron collector with platinum black in order to reduce secondary electron emission at the electron collector. The remainder of the tube parts is gold plated.

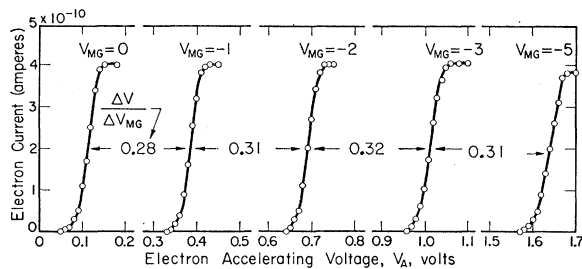


FIG. 2. Determination of the well depth by electron retarding (Tube type B). Electrons are retarded before entering the collision chamber, and collected at the electron collector, E , which is kept at +3.0 volts with respect to the collision chamber. The shift of the curves on the voltage axis is due to the penetration of the applied voltage, V_{MG} , into the center of the tube and equals the well depth, W .

The principle of the method has been described in Part I and will be only briefly summarized. An electron in the beam which makes an inelastic collision and whose residual energy is smaller than the well-depth voltage, is trapped in the axial direction by the electrostatic well. It cannot reach the collision chamber electrodes and will oscillate in the well until it finds its way to the trapped-electron collector, M . The collection mechanism is discussed in Sec. II of Part I.

II. DETERMINATION OF WELL DEPTH

It is desirable to establish accurately the well depth, W . This is done by three independent methods, namely the potential mapping of a scale size model of the tube in an electrolytic trough; by observing the shift in the threshold for positive ion production³ as a function of

³ The positive ion current is plotted against electron accelerating voltage (using the retarding potential difference method) from threshold to about 2 volts above threshold. This curve is extrapolated linearly to the voltage axis for each value V_{MG} . The shift

the potential between M and $G(V_{MG})$; and by observing the shift in the electron retarding curve⁴ when a negative potential is applied between M and G such that the electrons have to overcome a potential barrier.

The latter method is by far the simplest and fastest way to determine the well depth and it is used periodically to ascertain that the alignment of the grid and the cylinder M has not changed. A plot of the retarding curves at various values of V_{MG} is shown in Fig. 2. These data have been obtained with Tube B . Similar curves using Tube A show a broadening of the retarding curves which increases with an increasing value of V_{MG} . It is believed that electrons in Tube A do not pass through the exact center of the tube and thus a potential drop exists in the radial direction, across the electron beam. This effect is especially pronounced at a high well depth.

The well depth determined by the three methods described above should agree within experimental error. Figure 3 shows a plot of the well depth determined by the three methods vs the magnitude of the applied potential, V_{MG} , for Tube A . The agreement is seen to be most satisfactory.

III. ATOMIC EXCITATION—HELIUM

Energy Dependence of Cross Section

In order to check the operation of the tube with a deep well, the trapped-electron current is measured as a function of electron energy for helium. With a fixed well depth, W , we can trace out the excitation function by varying the electron accelerating voltage, V_A . This allows a determination of the excitation function between the onset of excitation, V_x , and (V_x+W) ; at an energy (V_x+W) , an artificial cutoff occurs due to the fact that electrons having suffered inelastic collisions now end up above the top of the well and are not trapped.

Alternatively, it is possible to keep the electron accelerating voltage fixed at a value below the first excitation potential and vary the well depth. The advantage of this method is the absence of an artificial cutoff; all inelastically scattered electrons are collected at all energies.⁵ Both these methods yield nearly identical results in atomic excitation (except for possible modifications discussed in the next section) but not in all cases of molecular excitation.

on the voltage axis results from the penetration of the voltage V_{MG} to the axis of the tube and is equal to the well depth. In this experiment the potential of M must be negative with respect to G so that positive ions can reach the ion collector, M .

⁴ Electrons are retarded as they enter the collision chamber and are collected at the electron collector E which is kept at a potential of about +3 volts with respect to the collision chamber electrodes. The shift of the inflection point of the retarding curve from that of the retarding curve taken with $V_{MG}=0$ is equal to the well depth W .

⁵ Above energies where ionization occurs this method measures directly the cross section (Q_x+2Q_i) where Q_x and Q_i are the excitation and ionization cross sections, respectively.

Figure 4 shows a comparison between the excitation cross section obtained by the trapped-electron method with the well depth fixed at 2.6 volts and by the "metastable production method."⁶ Both curves are normalized to unity at the peak of the 2³S excitation. The trapped-electron method shows a less pronounced dip at about 20.6 eV due to the poorer energy distribution of the electrons when using this method.⁷ The departure above 21.2 eV is presumably due to the excitation of the 2¹P resonance level which the metastable production method cannot measure. The shape of the excitation function of helium metastables determined by the trapped-electron method and the metastable production method is, therefore, identical within the limitations of each experiment. Since the latter method depends on the yield of electrons by metastable atoms in the 2³S and 2¹S states⁸ and the trapped electron method is independent of these secondary coefficients, it can be concluded that the yields of electrons by the incidence of metastable atoms in the 2³S and 2¹S states on a gold surface are identical. This finding is in agreement with theory.⁹

Magnitude of Cross Section

It was originally believed that the trapped-electron method would be a most reliable way of determining the magnitude of the cross section at the peak of the 2³S level. The method is independent of any secondary coefficients for metastable atoms and does not include transmission coefficients through grids since none of the trapped electrons are collected by the grid. In addition, it is easy to check the instrument by measuring positive ion production and thus calibrate the pressure gauge.¹⁰

Careful experiments under a variety of operating conditions and with both types of tubes (A, B) show that the cross section measured by the trapped-electron method at the peak of the 2³S level is larger than the accepted value of 5×10^{-18} cm² given by Maier-Leibnitz.¹¹ In fact, the measured cross section at a fixed

⁶ In the metastable production method, the secondary electrons due to the arrival of metastable atoms at a metal surface are measured. See reference 2 and R. Dorrestein, *Physica* **9**, 447 (1942).

⁷ Although the electron beam reaching the collision chamber has an energy spread of the order of 0.1 eV, it will acquire a larger effective energy spread due to the nonrectangular shape of the potential well.

⁸ The excitation function obtained by the metastable production method is due primarily to the 2³S and 2¹S states in the energy range shown in Fig. 4. The position of the second peak on the energy scale makes it improbable that it can be due to the 2³P state as recently postulated (S. J. B. Corrigan and A. Von Engel, *Proc. Phys. Soc. (London)* **72**, 786 (1958). Further proof that the second peak results from the 2¹S state is given in Part I where it is shown that the slope of the excitation function for the 2¹S state near threshold is three times larger than the slope for the 2³P excitation function near threshold.

⁹ H. Hagstrum, *Phys. Rev.* **91**, 543 (1953); L. J. Varnerin, *Phys. Rev.* **91**, 859 (1953).

¹⁰ In the present experiment, a correction of 7% was necessary to bring the positive ion cross section into agreement with that given by P. T. Smith, *Phys. Rev.* **36**, 1293 (1930).

¹¹ H. Maier-Leibnitz, *Z. Physik* **95**, 499 (1936).

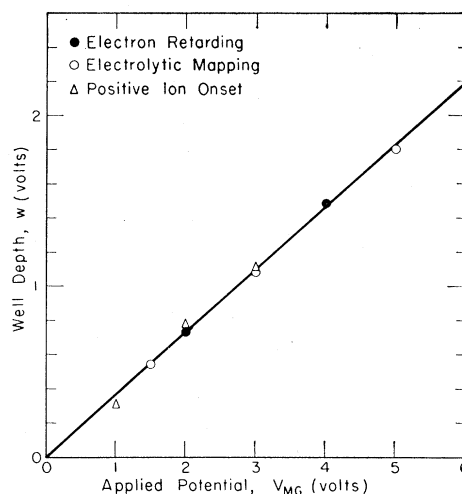


FIG. 3. Well depth vs applied potential, V_{MG} , determined by the three methods indicated on the graph. In the geometry used, thirty-seven percent of the potential applied between M and G penetrates to the axis of the tube. These data are obtained with Tube A and an electrolytic analog of the same.

electron energy (peak of the 2³S excitation) increases with increasing well depth despite the linear dependence of the measured current with pressure. The discrepancy is 14% at a well depth of 0.69 volt and 50% at 1.6 volts.

The dependence of the measured cross section on well depth is believed to be caused by those electrons in the beam which have made elastic collisions. These electrons maintain their original energy but their velocity vectors are reoriented. Those electrons whose velocity is nearly perpendicular to the axis of the tube

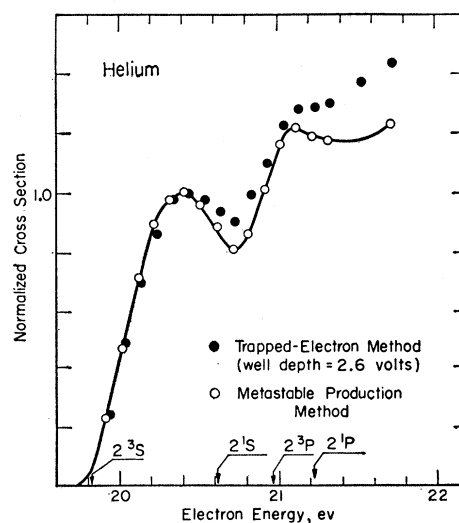


FIG. 4. Excitation function in helium. The closed circles are data obtained by the trapped-electron method and the open circles are data obtained by the metastable production method. The discrepancies between the two methods are discussed in the text. Both curves are normalized to unity at the peak of the 2³S excitation.

are now trapped until another collision reorients their velocity in the axial direction, such that they can reach the electron beam collector or the collision chamber electrodes. These elastically scattered electrons do not reach the trapped electron collector because many collisions are necessary to diffuse there. However, the elastically scattered electrons essentially increase the effective path length. They make many traversals parallel to the axis of the tube and are measured on the electron collector only once. The fraction of elastically scattered electrons trapped in the tube depends on (W/U) , the ratio of well depth to the total electron energy, U , and the angular distribution of elastically scattered electrons.¹² Since the shape of the angular distribution is not known accurately, it is not known at present how to extrapolate absolute cross-section data to zero well depth.

IV. MOLECULAR ELECTRONIC EXCITATION—NITROGEN

When applying the trapped-electron method to molecular electronic excitation one must distinguish between two limiting cases, namely, (a) transitions to a repulsive-type state in which the potential curve for the state traverses the Franck-Condon region over an energy range much larger than the well depth, and (b) transitions to a bound state. In case (a) we trace out the integral of the cross section for production of electrons with kinetic energy from 0 to W (ev) resulting from transitions from the ground state to the repulsive state within the Franck-Condon range. (See Part I, Sec. V.) Case (b) resembles the excitation to atomic

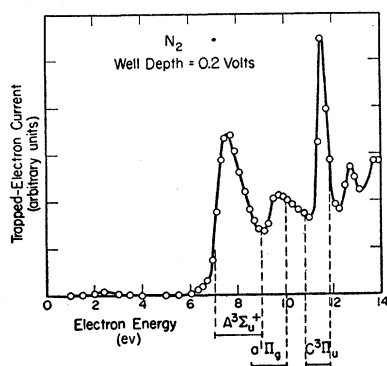


FIG. 5. Excitation spectrum of nitrogen using a well depth of 0.2 volt. The Franck-Condon range of a few states of the nitrogen molecule is indicated.

¹² If we assume that the confined elastically scattered electrons have a path length in the collision chamber equal to their mean free path, then the measured cross section, Q_M , can be related to the true cross section, Q , by the relation $Q_M = Q[1 + (W/U)^n]$ where W is the well depth and U is the electron energy. The exponent, n , depends on the angular distribution of elastically scattered electrons. For an isotropic distribution, we have $n=0.5$. However, an anomalous angular distribution of elastically scattered electrons could occur near the peak of the 2^3S level in view of the suggestion of E. Baranger and E. Gerjouy [Proc. Phys. Soc. (London) **72**, 326 (1958)] that a compound state exists in that energy range.

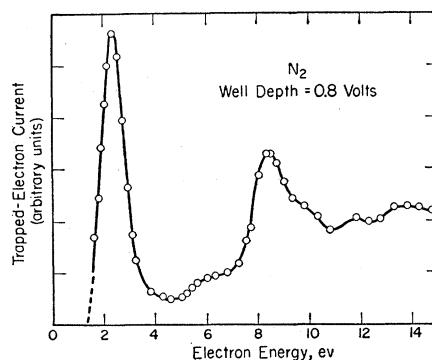


FIG. 6. Excitation spectrum of nitrogen using a well depth of 0.8 volt.

levels (as discussed above for helium) if a given vibrational state is preferentially excited. This condition is fulfilled when the minimum of the potential curve for the excited state lies at approximately the same internuclear separation as the minimum of the potential curve for the ground state.

Figure 5 shows the results obtained in N_2 with a fixed well depth of 0.2 volt. In this case, only electrons with kinetic energy in the range 0–0.2 ev contribute to the trapped-electron current. Four distinct peaks occur below 12 ev. The first, at 2.3 ev, will be discussed in the next section. The second, with an onset above 6.0 ev, is associated with the $A^3\Sigma_u^+$ state, which is the lowest electronically excited state of the nitrogen molecule. The potential curve for this state traverses the Franck-Condon region over an energy range of 4 ev,¹³ and thus fulfills our definition of a repulsive-type state. The second peak results from the $\sigma^1\Pi_g$ and other states in that energy range. The onset at 11.2 ev (with a peak at 11.5 ev) coincides energetically with the excitation of the $C^3\Pi_u$ state. An examination of the potential curve for the C state shows¹³ that the potential minimum occurs at almost the same internuclear separation as the minimum of the ground state. Thus, we must consider the C state an atomic-type excitation process.

Figure 6 shows the trapped-electron current *vs* electron energy at a well depth of 0.8 volt. The absence of a peak due to the C state should be noted. It is an indication that the excitation function for the C state peaks less than 0.8 ev above threshold. This finding is confirmed by recent optical experiments.¹⁴

V. LOW-ENERGY INELASTIC PROCESS—NITROGEN

The most striking feature of the curve in Fig. 5 is the peak with a maximum at 2.3 ev. This low-energy loss

¹³ For a diagram of potential energy curves for nitrogen, see W. Lichten, J. Chem. Phys. **26**, 306 (1957). Higher states could contribute to the first peak of Fig. 4 above 7.5 ev, but the lack of a break in the curve suggests that the cross section for these higher states must be smaller near threshold than for the $A^3\Sigma_u^+$ state.

¹⁴ D. T. Stewart and E. Gabathuler, Proc. Phys. Soc. (London) **72**, 287 (1958).

process in nitrogen was first observed by Haas¹⁵ in a swarm experiment. The inelastic cross section shown in Fig. 6 does not result from any known electronically excited states of the nitrogen molecule since the first electronically excited level, $A^3\Sigma_u$, lies above 6.0 eV. Haas has also pointed out that the "direct" excitation of vibrational states of the nitrogen molecule by electron impact is improbable.¹⁶ Only when the incoming electron spends a time long compared to the vibration time in the vicinity of the molecule can the cross section for vibrational excitation be appreciable. This leads to the hypothesis that a temporary negative ion state of the nitrogen molecule exists around 2.3 eV.

A sharp increase in the total cross section at 2.3 eV in nitrogen has been observed in Ramsauer type experiments,¹⁷ and has been interpreted theoretically by Fisk¹⁸ as being due to an elastic process. His calculation gives a peak in the elastic cross section at 2.5 eV and a subsidiary rise at 5.0 eV. Since the resonance behavior in elastic and inelastic processes is related it is possible that Fisk's elastic resonance process is a manifestation of the existence of the nitrogen negative ion state.

The curve of Fig. 6 exhibits a rise at 5.0 eV, and it is possible that this increase in the inelastic cross section results from a higher negative-ion state. Fisk's calculation of the elastic cross section shows a similar rise at about 5.0 eV, but the cross section obtained by Ramsauer-type experiments remains flat in that energy

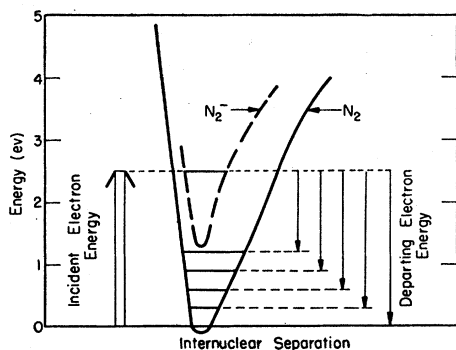


FIG. 7. Hypothetical diagram of the negative-ion state of nitrogen. The energy scale is chosen to conform to the experimental evidence. The negative ion presumably decays to various vibrational levels of the neutral molecule.

¹⁵ R. Haas, *Z. Physik* **148**, 177 (1957).

¹⁶ In order to explain the phenomena observed in the present experiment (and also in Haas' experiment) one would have to postulate the excitation of high-lying vibrational states by the incoming electron. However, in "direct" excitation, the time spent by the incoming electrons in the neighborhood of the molecule is about 100 times smaller than the vibration time. Under these conditions, the excitation of vibrational levels is not appreciable. (See H. S. W. Massey and E. H. S. Burhop, *Electronic and Ionic Impact Phenomena* (Clarendon Press, Oxford, 1952), p. 454.

¹⁷ For a review, see H. S. W. Massey and E. H. S. Burhop, *Electronic and Ionic Impact Phenomena* (Clarendon Press, Oxford, 1952), p. 206.

¹⁸ J. B. Fisk, *Phys. Rev.* **49**, 167 (1936). See also reference 17, p. 214.

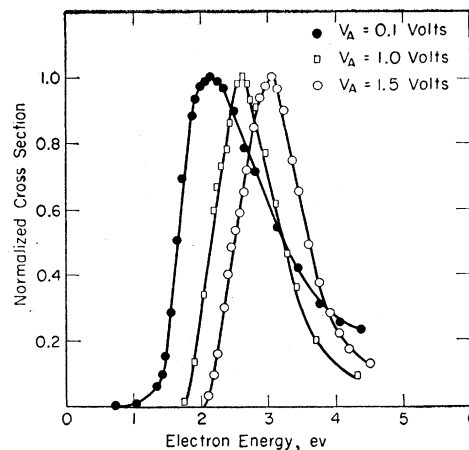


FIG. 8. Low-energy inelastic process in nitrogen. The data are obtained by keeping the accelerating voltage, V_A , at the values indicated on the graph and changing the well depth, W . The electron energy is equal to $V_A + W$. All curves are normalized to unity at their peak. The relative magnitudes of the curves and the cause for the shift are discussed in the text.

range. Regarding the magnitude of the inelastic cross section at 2.3 eV, Haas gives a value of 15% of the elastic cross section, i.e., 3×10^{-16} cm². In view of the difficulties with absolute cross-section measurements described in Sec. III, no attempt was made to determine the magnitude of this cross section.

Interpretation of the Trapped-Electron Method for the Low-Energy Loss Process in Nitrogen

Figure 7 shows a hypothetical diagram of the temporary negative-ion state and the ground state of nitrogen. The energy scale and the general shape of the negative-ion state are chosen so as to conform to the experimental evidence. On this model, the incident electron excites the negative-ion state and the compound molecule decays to the various vibrational states of the neutral molecule.¹⁹ The two possible measurements of the energy dependence of the cross section, namely, with a fixed well depth or a fixed accelerating voltage, do not give the same curve on a model such as Fig. 7. With a constant accelerating voltage fixed at V_A , and the remainder of the electron energy supplied by the well depth, W , we collect those electrons that have a residual energy between 0 and W (eV). However, the residual energy of the electrons is equal to the difference between the incident electron energy, $V_A + W$, and the vibrational energy of the molecule. Thus, with a fixed V_A we measure only those processes which have left the molecule in a vibrational state in excess of V_A . It follows that with V_A equal to 0.1 volt, all inelastic processes are measured (the vibrational spacing is approximately 0.3 eV), whereas with V_A equal to 1.0 volt,

¹⁹ The incident electron does not suffer any energy loss if the negative ion relaxes to the ground vibrational state; this type of collision is indistinguishable from an elastic collision.

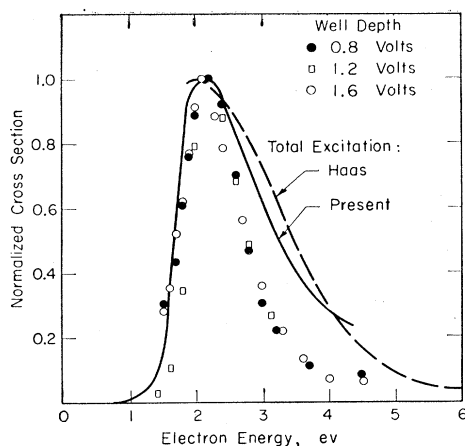


FIG. 9. Comparison of the peak shape of the low-energy inelastic process in nitrogen obtained by various methods. The dashed curve is Haas' result in a swarm experiment, the solid curve is replotted from Fig. 9 (constant accelerating voltage, $V_A=0.1$ volt). The experimental points are obtained by varying the accelerating voltage and keeping the well depth fixed at the values indicated on the graph. The points lie below the "total" curves because of the relatively lower probability of exciting high vibrational states.

only those states which have a vibrational energy in excess of 1 eV above the ground state contribute. Figure 8 shows the experimental results for V_A equal to 0.1, 1.0, and 1.5 volts. All curves are normalized to unity at their peak. Actually the cross section at the peak of the 0.1-volt curve is twenty times higher than the peak of the 1.5-volt curve. This decrease in peak height can be ascribed not only to the decrease in the number of states included in the 1.5-volt curve but also to the fact that the cross section for production of high-lying vibrational states is low.²⁰ The shift on the energy scale of the curves in Fig. 8 is attributed to the relatively higher probability of exciting high vibrational states with the faster electrons. The overlap integral between the high vibrational states of N_2^- and high vibrational states of N_2 is higher than the overlap of low vibrational states of N_2^- with high vibrational states of N_2 . Haas observed that the energy distribution of the electrons after inelastic excitation in his swarm experiment is peaked around 1.5 eV, independent of the incident electron energy, in the energy range from 2.7 eV to 5.2 eV. A tendency toward a constant value for the departing electron energy is to be expected from the above considerations (at higher incident energies there is a trend toward excitation of higher vibrational levels and, therefore, the departing electron energy tends to remain constant).

Figure 9 shows, on a normalized scale, a comparison of the data obtained in the present experiment with

²⁰ The smaller population of the higher vibrational levels is the reason for the very small effect seen at 2.3 eV in Fig. 5, where a small well depth is used, i.e., only high-lying vibrational states are included.

$V_A=0.1$ volt (total excitation) with Haas' experimental data. The agreement is seen to be good. The experimental points shown in Fig. 9 are obtained with a well depth fixed at the three values indicated in the figure and varying the accelerating voltage, V_A . In this type of experiment, the trap depth determines the number of vibrational states included in the experiment. Thus, with $W=0.8$ volt, approximately three vibrational states contribute to the experiment. As the electron energy is increased by increasing V_A , states lying higher above the ground state will be included and lower states will be excluded. If the cross sections for production of various vibrational states were equal, the points should lie on the curves marked "total excitation" in Fig. 9. The fact that the points lie considerably below the curves, especially at the higher energies, is taken as a further indication that the cross section for production of high vibrational states is smaller than the cross section for the low states. The elastically scattered electrons trapped in the tube discussed in Sec. III may influence the shape of the curves shown in Fig. 9. However, the ratio W/U remains almost constant (near unity) for the "total excitation" curve of Fig. 9 so that elastically confined electrons may not influence the shape of the curve.

VI. RESULTS IN CO, H₂, O₂

The results obtained in carbon monoxide are shown in Fig. 10 for a well depth of 0.7 volt. The inelastic cross section has a behavior very similar to that observed in nitrogen, including the low-energy peak which occurs at a slightly lower energy (1.7 eV) in CO than in N_2 . The onset of the $a^3\Pi$ state in CO occurs at lower energies than the $A^3\Sigma$ state in N_2 . The similar behavior of CO and N_2 is expected since the two molecules are iso-electronic. A search for low-energy inelastic processes in H_2 and O_2 by the same methods as used in N_2 and CO showed no pronounced peaks similar to those observed at 2.3 eV in N_2 . An inelastic process is observed using a large well depth in H_2 . The shape of this peak is similar to the 5-eV process observed in N_2

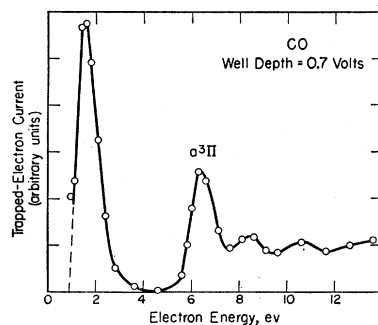


FIG. 10. Excitation spectrum of carbon monoxide using a well depth of 0.7 volt.

(see Fig. 6), except that the broad onset occurs around 3.5 ev.

ACKNOWLEDGMENTS

The author is indebted to the members of the Atomic Physics Group of the Westinghouse Research Labora-

tories for many helpful discussions of the problems involved. Especially, thanks are due to A. V. Phelps and T. Kjeldaas for advice freely given during the course of this work and for discussion of the many pitfalls which had to be overcome before the trapped-electron method yielded usable data.

PHYSICAL REVIEW

VOLUME 116, NUMBER 5

DECEMBER 1, 1959

Sauter Theory of the Photoelectric Effect*

U. FANO, *National Bureau of Standards, Washington, D. C.*
K. W. McVoy,† *Brookhaven National Laboratory, Upton, New York*

AND

JAMES R. ALBERS, *National Bureau of Standards, Washington, D. C.*
(Received January 30, 1959)

Results of Sauter are expressed in the form of a transition matrix which determines the photoelectric effect cross section for arbitrary x-ray polarization and arbitrary initial and final orientations of the electron spin. The structure of the matrix elements accounts for curious properties of the cross section in terms of interference between orbital and spin currents. Expansion of the wave functions into powers of $Z/137$ simplifies the calculation of the transition matrix, reduces it to a special case of the bremsstrahlung theory in Born approximation, and explains discrepancies between results of earlier calculations. Analytical and graphical data are given on the photoemission of polarized electrons by circularly polarized x-rays.

1. INTRODUCTION

UNCERTAINTIES regarding the significance of theoretical results on the photoelectric effect and discrepancies between experimental results have stimulated an effort to clarify the content of the theory and to develop further its application. In the course of this work it has emerged that the theories of the photoelectric effect and of bremsstrahlung coincide, in essence, to lowest order in $Z/137$. This paper reports the results of analysis and calculations on the photoelectric effect. Separate papers deal with the mathematical justification of the expansion which establishes the connection with bremsstrahlung,¹ with applications of this connection²⁻⁴ and with a detailed analysis of spin effects in the absorption or emission of radiation.⁵

An important relativistic calculation of the cross section for the photoelectric effect in the K shell of atoms was carried out by Sauter in 1931.^{6,7} The calculation involved an expansion into powers of the atomic

number Z and has accordingly often been classed as a Born approximation, although this term is properly applied in a more restricted sense. Because Sauter did not follow the usual rather simple method of Born approximation calculations, his results are not physically transparent.⁸ Sauter himself felt unable to "read out" of his calculation results on the probability of electron spin reorientation which were implicitly contained in it (reference 7, p. 485). Spin orientation and its relation to circular polarization of the x-rays have attracted increasing attention in recent years,⁹ and will be considered in some detail in this paper.

It may be noted that the integral cross sections for the photoelectric effect calculated by Sauter for high- Z materials exceed by a factor ~ 2 those obtained numerically by Hulme *et al.*, with exact Coulomb-field wave functions^{10,11} and those obtained experimentally at relativistic energies. (The discrepancy is much larger still at lower energies, e.g., at 50 kev.) On the other hand, the Hulme procedure has never been applied extensively or to verify whether any of the more

* Supported by the Office of Naval Research and the U. S. Atomic Energy Commission.

† Present address: Brandeis University, Waltham, Massachusetts.

¹ K. W. McVoy and U. Fano, this issue [Phys. Rev. **116**, 1168 (1959)].

² U. Fano, following paper [Phys. Rev. **116**, 1156 (1959)].

³ Fano, Koch, and Motz, Phys. Rev. **112**, 1679 (1958).

⁴ J. W. Motz and R. C. Placious, Phys. Rev. **112**, 1039 (1958).

⁵ Fano, McVoy, and Albers, this issue [Phys. Rev. **116**, 1159 (1959)].

⁶ F. Sauter, Ann. Physik **9**, 217 (1931).

⁷ F. Sauter, Ann. Physik **11**, 454 (1931).

⁸ An independent derivation of Sauter's results by A. Sommerfeld, *Atombau und Spektrallinien* (F. Vieweg und Sohn, Braunschweig, 1939), second edition, Vol. 2, p. 482 ff., proved of little advantage in this respect.

⁹ See in particular, K. W. McVoy, Phys. Rev. **108**, 365 (1957).

¹⁰ Hulme, McDougall, Buckingham, and Fowler, Proc. Roy. Soc. (London) **149**, 454 (1935).

¹¹ See in particular, W. Heitler, *Quantum Theory of Radiation* (Oxford University Press, Oxford, 1954), third edition, p. 209 ff.